

Electronic Supplementary Information for A Molecular Dynamics Investigation Of Actinyl-Ligand Speciation In Aqueous Solution

Ken Newcomb,[†] Surya Prakash Tiwari,^{‡,¶} Neeraj Rai,[§] and Edward J. Maginn^{*,†}

[†]*Department of Chemical and Biomolecular Engineering, 182 Fitzpatrick Hall, University of
Notre Dame, Notre Dame, IN 46556, USA*

[‡]*U. S. Department of Energy, National Energy Technology Laboratory, Pittsburgh, PA 15236,
USA*

[¶]*AECOM, South Park, PA 15129, USA*

[§]*Dave C. Swalm School of Chemical Engineering, Mississippi State University, Mississippi State,
MS, USA 39762*

E-mail: ed@nd.edu

Phone: 01 574 631 5687. Fax: 01 574 631 8366

1 **Supplementary Information**

2 **Development of Force Field Parameters from Quantum-Mechanical (QM)**

3 **Calculations**

4 QM calculation details are described in our previous works.^{1,2} To summarize, uranyl ion was sol-
5 vated with 3 or 4 water molecules depending on the bidentate or monodentate ligand, respectively,
6 and the 4th or 5th water molecule was moved by varying the distance between U and an atom of

7 the ligand with three different configurations as shown in Fig. S1. All configurations are the same
 8 as those used in our previous work² except CONF2. Previously used CONF2 was very repulsive
 9 and thus was not a very useful PES. The CONF2 used in this work is attractive and will add quality
 10 to the force field parameters derived from fitting the PESs.

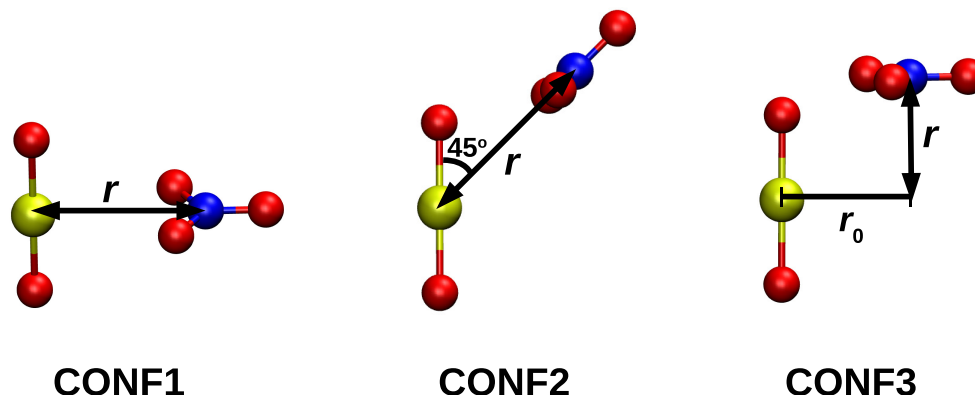


Figure S1: Configurations used for generating QM potential energy surfaces, shown for NO_3^- . The actinyl ion is solvated by four or three water molecules (not shown for clarity), depending on the monodentate (such as F^- , Cl^- , OH^- , Na^+) or bidentate ligand (NO_3^- , CO_3^{2-} , SO_4^{2-}), respectively. In CONF3, r_0 is kept constant during the scan, and its value is given by a equilibrium distance obtained from the optimization.

11 During the scan, all atoms were kept frozen except the distance between actinyl ion and the
 12 ligand. Initial structures were obtained from optimizing the whole structure. The QM- MP2 inter-
 13 action energy between actinyl ion and the ligand is given by^{1,2}

$$U_{\text{CONF},i}^{\text{QM}} = \{E[\text{UO}_2^{2+} + \text{XW} + \text{Ligand}] - E[\text{UO}_2^{2+} + \text{XW}] - E[\text{Ligand}]\} \\ - \{E[\text{XW} + \text{Ligand}] - E[\text{XW}] - E[\text{Ligand}]\}$$

or, $U_{\text{CONF},i}^{\text{QM}} = E[\text{UO}_2^{2+} + \text{XW} + \text{Ligand}] - E[\text{UO}_2^{2+} + \text{XW}] - E[\text{XW} + \text{Ligand}] + E[\text{XW}]$ (1)

14 where $E[\text{Y}]$ represents the QM energy of species Y computed with all the basis functions.
 15 Counterpoise calculations were done by setting up ghost atoms which have normal basis sets, but
 16 no electrons or nuclear charge. For eg., atoms of UO_2^{2+} were treated as ghosts atoms for the

17 calculation of $E[\text{XW} + \text{Ligand}]$.

18 A Python code was written to fit the QM PES to Lennard-Jones (LJ) + Coulombic potential
19 functional form. For fitting, the objective function (O) used for minimization is:

$$O = \sum_{\text{CONF}} \sum_i (U_{\text{CONF},i}^{\text{QM}} - U_{\text{CONF},i}^{\text{Cl}}) \exp(-\beta U_{\text{CONF},i}^{\text{QM}}) \quad (2)$$

20 where, $U_{\text{CONF},i}^{\text{QM}}$ and $U_{\text{CONF},i}^{\text{Cl}}$ are QM and classical potential energies, respectively, at different points
21 i (different distances between U and Ow) for a given configuration CONF. $\exp(-\beta U_{\text{CONF},i}^{\text{QM}})$ is
22 used as a weighing factor to weigh the lower energies more. The value of β was determined by
23 empirical adjusting it and improving the quality of fits by minimizing the objective function O as
24 well as visually inspecting the quality of fits. β equal to 0.025 mol/kJ was found appropriate for
25 the present case. Figures S3-S8 show a comparison of the PESs generated from QM alongside the
26 classical fits and literature values. In addition, they show the PMF obtained by the classical fits
27 compared to PMF generated by using the literature's parameters.

28 **FFP Validation**

29 First, we compare the PMF plots and the stability constants for uranyl ion obtained from using
30 FFPs from QM PES vs. FFPs from literature. Let the FFPs and PMFs from QM fits be designated
31 as QM FFPs and QM PMFs, respectively. The terms Lit FFPs and Lit PMFs refer to values
32 obtained using FFPs from the literature. Plots of QM and Lit FFPs and corresponding PMFs for
33 the F^- anion are shown in Fig. S2. The QM PESs are consistently more attractive compared to the
34 corresponding Lit PESs, which is reflected in the PMF plots. We attribute the high ligand attraction
35 seen in the QM PESs and PMFs to the fact that though the uranyl ion was solvated during the QM
36 calculations, anions were left bare, which can increase the interaction energy between the two
37 groups. We tried to correct this effect by scaling down the anion charges, but it worked only for
38 monodentate ligands. Charge scaling had no effect on bidentate ligands, for which the whole QM
39 PES should be scaled down first.

40 PESs derived from QM calculations were compared to the PESs obtained from using literature
 41 ligand parameters and applying mixing rules. In addition, the potential of mean force (PMF)
 42 was calculated between actinide ion and the ligand for both sets of FFPs. The PESs generated
 43 from literature FFPs are consistently higher in energy compared to QM PESs. While the QM
 44 calculations used a solvated actinyl ion, the ligand was left bare, causing a strong actinide-ligand
 45 association. If the For this reason, it was decided to use the literature FFPs for the study. Both sets
 46 of parameters can be found in Table S1. The PMFs generated with our QM-PES parameters were
 47 calculated using the umbrella sampling technique - all other PMFs were calculated using ABF.

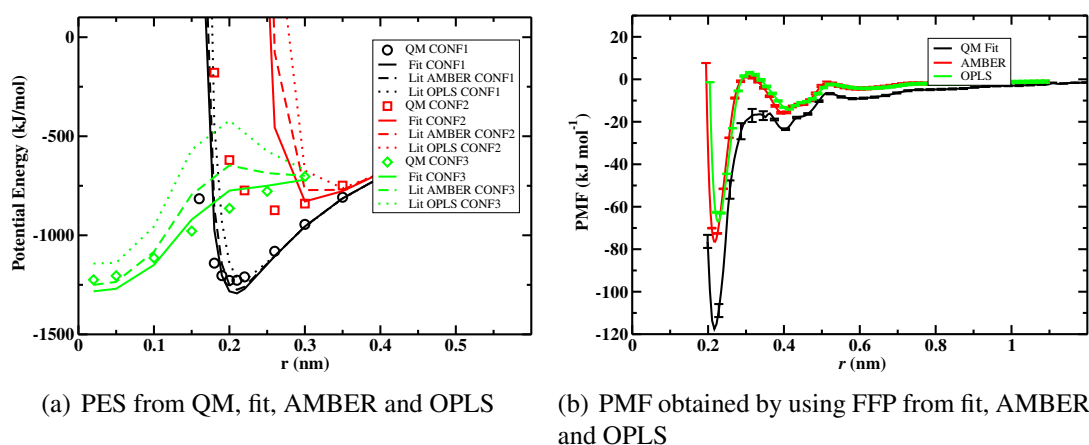


Figure S2: PESs and PMFs for UO_2^{2+} - F^- interaction

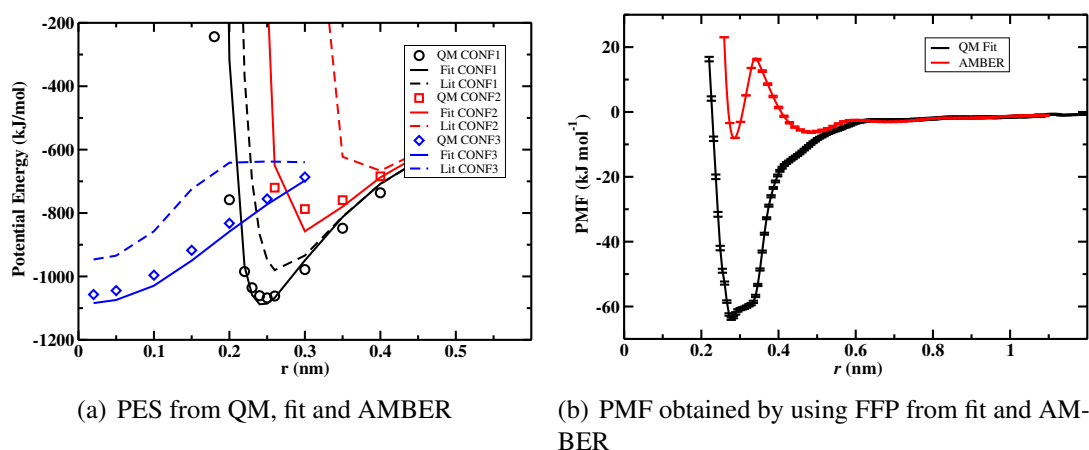
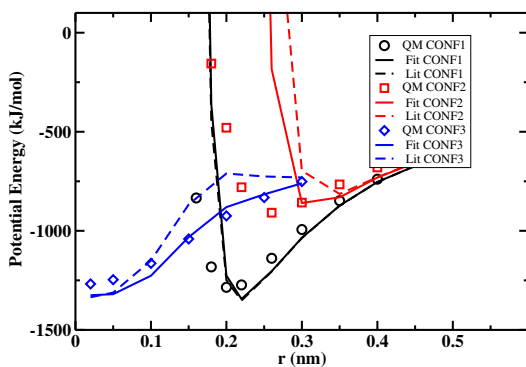
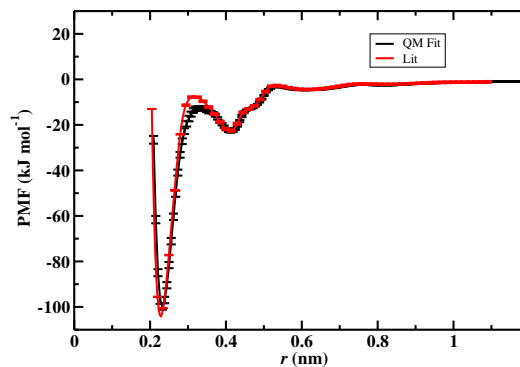


Figure S3: PESs and PMFs for UO_2^{2+} - Cl^- interaction

48 Figure S9 shows the switching function used in our polyionic study, along with the values of

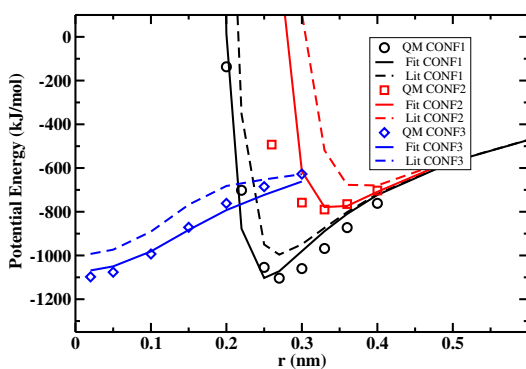


(a) PES from QM, fit and literature

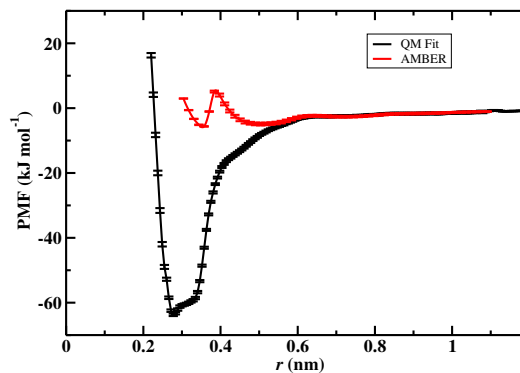


(b) PMF obtained by using FFP from fit and literature

Figure S4: PESs and PMFs for UO_2^{2+} - OH^- interaction

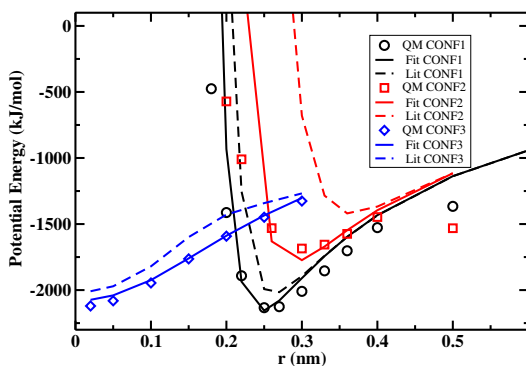


(a) PES from QM, fit and literature

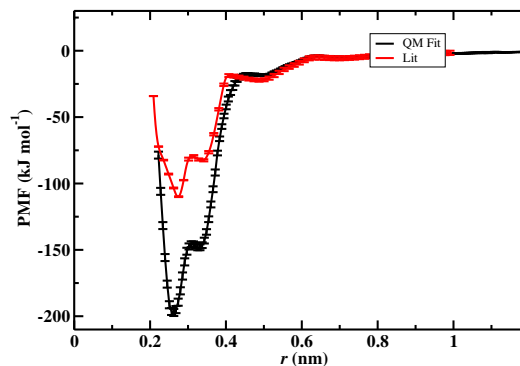


(b) PMF obtained by using FFP from fit and literature

Figure S5: PESs and PMFs for UO_2^{2+} - NO_3^- interaction



(a) PES from QM, fit and literature



(b) PMF obtained by using FFP from fit and literature

Figure S6: PESs and PMFs for UO_2^{2+} - CO_3^{2-} interaction

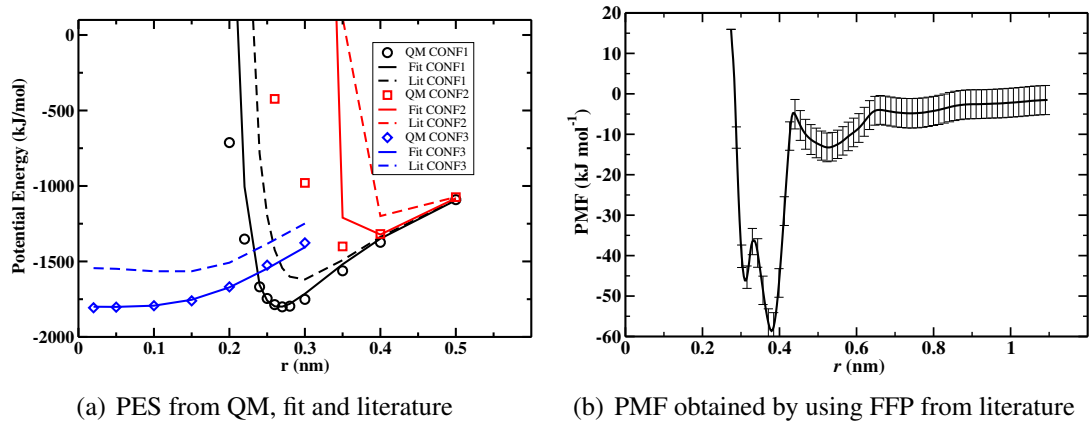


Figure S7: PESs and PMF for UO_2^{2+} - SO_4^{2-} interaction

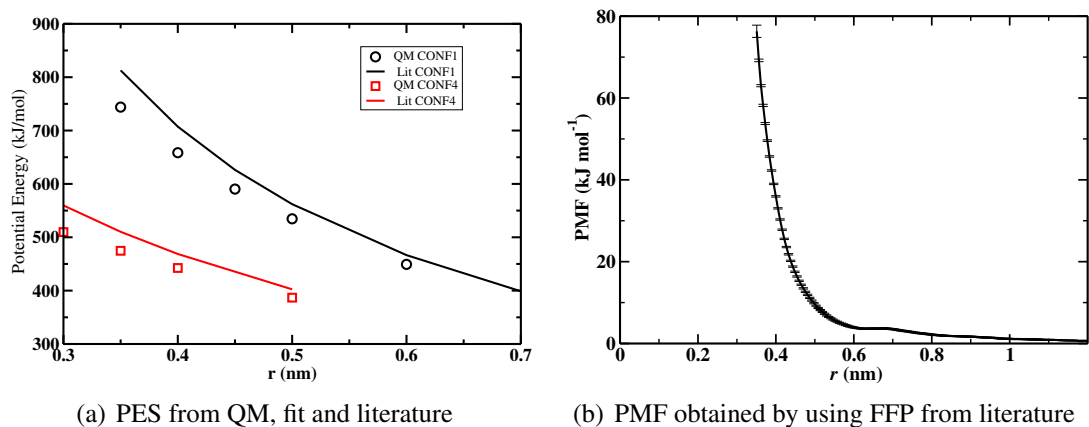


Figure S8: PESs and PMF for UO_2^{2+} - Na^+ interaction

Table S1: Force field parameters for ligands, obtained from the literature and from fitting quantum-mechanical potential energy surfaces

Ion	Atom	Charge	$\sigma_{\text{AnL}}^{\text{Lit}}$ (nm)	$\sigma_{\text{AnL}}^{\text{QM}}$ (nm)	$\epsilon_{\text{AnL}}^{\text{Lit}}$ (kJ/mol)	$\epsilon_{\text{AnL}}^{\text{QM}}$ (kJ/mol)
F ⁻ ^a	F	-1	0.303	0.316	0.367	0.200
F ⁻ ^b	F	-1	0.284	0.316	1.264	0.200
Cl ⁻ ^a	Cl	-1	0.368	0.367	0.471	0.200
Na ⁺ ^a	Na	1	0.314	N/A	0.078	N/A
NO ₃ ⁻ ^c	N	0.626	0.313	0.278	0.596	2.500
	O	-0.542	0.294	0.245	0.577	2.500
OH ⁻ ^d	O	-1.4238	0.306	0.337	0.587	0.200
	H	0.4238	0	0	0	0
SO ₄ ²⁻ ^e	S	2.4	0.325	N/A	0.745	N/A
	O	-1.1	0.305	N/A	0.745	N/A
CO ₃ ²⁻ ^f	C	1.1230	0.286	0.332	0.357	0.200
	O	-1.0410	0.306	0.312	0.587	0.200

^aAMBER FFP. ³

^bOPLS FFP. ⁴

^cGuilbaud et al.,^{5,6} along with an improper dihedral of the form $V_{id}(\xi_{ijkl}) = \frac{1}{2}k_{\xi}(\xi_{ijkl} - \xi_0)^2$ was used, where $\xi_0 = 0^\circ$ and $k_{\xi} = 481.6$ kJ/mol/rad² derived from QM calculations.

^dBrodskaya et al.⁷. Rigid ion model. O-H distance = 0.1 nm.

^eWernersson et al.⁸. Rigid ion model. O-S distance = 0.14898 nm.

^fWang et al.⁹ GM rules were used for interactions between the atoms of CO₃²⁻ - water, and CO₃²⁻ - actinyl ions. Harmonic bond O-C: $U_b = \frac{1}{2}c_0(b - b_0)^2$ with $b_0 = 0.13$ nm, $c_0 = 644336.0$ kJ/mol/(nm)²; Harmonic angle O-C-O: $U_{\theta} = \frac{1}{2}c_0(\theta - \theta_0)^2$ with $\theta_0 = 120^\circ$, $c_0 = 920.5$ kJ/mol/(rad); Harmonic improper dihedral C-O3: $V_{id}(\xi_{ijkl}) = \frac{1}{2}k_{\xi}(\xi_{ijkl} - \xi_0)^2$ with $\xi_0 = 0^\circ$, $k_{\xi} = 2100$ kJ/mol/rad².

49 the parameters.

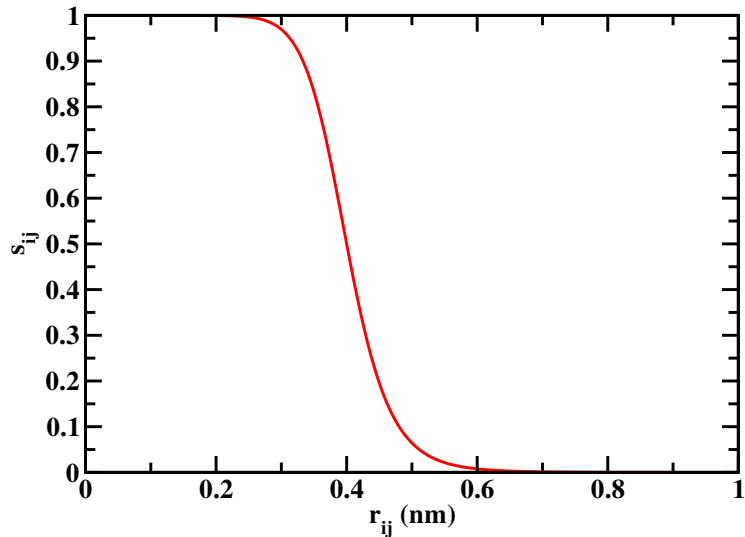


Figure S9: The switching function used for the polychloride association study, with $d_0 = 0$, $r_0 = 0.4$ nm, $n = 12$, and $m = 24$.

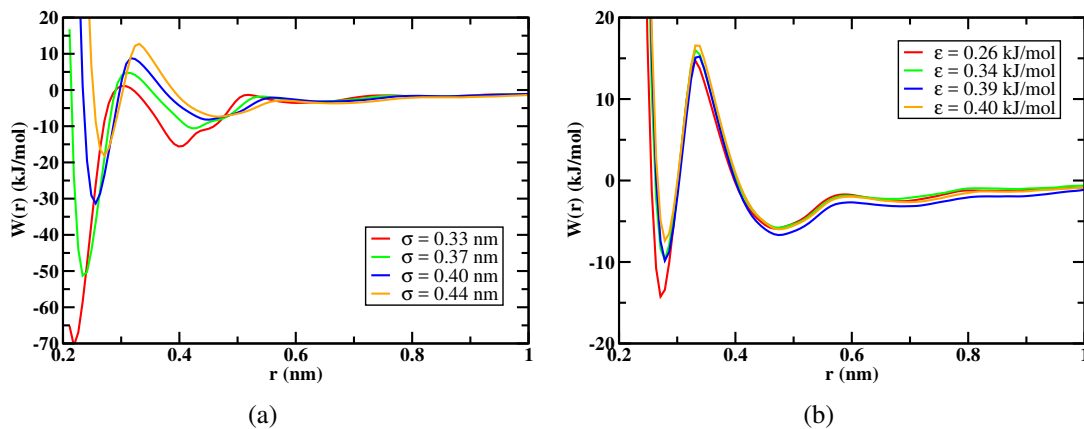


Figure S10: A study on the effect of σ and ϵ on the strength of ligand binding. (a) ϵ for Cl^- is held constant, while σ is varied. (b) σ for Cl^- is held constant, while ϵ is varied.

Table S2: TST rate constants and transmission coefficients for actinyl-ligand CIP dissociation.

Ligand	FFP	$k_{UO_2^{2+}}^{TST}$ (s ⁻¹)	$k_{NpO_2^+}^{TST}$ (s ⁻¹)	$\kappa_{UO_2^{2+}}$ (s ⁻¹)	$\kappa_{NpO_2^+}$ (s ⁻¹)
F ⁻	AMBER	4.9×10^{-1}	1.7×10^6	0.254 ± 0.013	0.241 ± 0.018
	OPLS	1.1×10^1	2.2×10^6	0.257 ± 0.016	0.234 ± 0.025
OH ⁻	Literature	2.9×10^{-4}	3.7×10^4	0.184 ± 0.007	0.156 ± 0.015
CO ₃ ²⁻	Literature	1.6×10^{-3}	9.6×10^4	0.090 ± 0.013	0.059 ± 0.029
SO ₄ ²⁻	Literature	1.9×10^3	1.0×10^{10}	0.064 ± 0.005	0.083 ± 0.015
NO ₃ ⁻	Literature	3.8×10^{10}	1.7×10^{10}	0.118 ± 0.153	0.069 ± 0.014
Cl ⁻	AMBER	4.6×10^8	2.8×10^{10}	0.033 ± 0.003	0.262 ± 0.019
H ₂ O	SPC/E	6.1×10^9	8.2×10^9	0.128 ± 0.011	0.159 ± 0.016

References

- 51 (1) Rai, N.; Tiwari, S. P.; Maginn, E. J. *J. Phys. Chem. B* **2012**, *116*, 10885–10897.
- 52 (2) Pomogaev, V.; Tiwari, S. P.; Rai, N.; Goff, G. S.; Runde, W.; Schneider, W. F.; Maginn, E. J.
53 *Phys. Chem. Chem. Phys.* **2013**, *15*, 15954–63.
- 54 (3) Wang, J.; Wolf, R. M.; Caldwell, J. W.; Kollman, P. A.; Case, D. A. *J. Comput. Chem.* **2004**,
55 *25*, 1157–74.
- 56 (4) Jorgensen, W. L.; Maxwell, D. S.; Tirado-Rives, J. *J. Am. Chem. Soc.* **1996**, *118*, 11225–11236.
- 57 (5) Guilbaud, P.; Wipff, G. *J. Phys. Chem.* **1993**, *97*, 5685–5692.
- 58 (6) Guilbaud, P.; Wipff, G. *J. Mol. Struct. THEOCHEM* **1996**, *366*, 55–63.
- 59 (7) Brodskaya, E.; Lyubartsev, A. P.; Laaksonen, A. *J. Phys. Chem. B* **2002**, *106*, 6479–6487.
- 60 (8) Wernersson, E.; Jungwirth, P. *J. Chem. Theory Comput.* **2010**, *6*, 3233–3240.
- 61 (9) Wang, J.; Becker, U. *Am. Mineral.* **2009**, *94*, 380–386.